COUPLED LONGITUDINAL AND TRANSVERSE BEAM DYNAMICS STUDIES FOR HADRON THERAPY LINACS

R. Apsimon*, G. Burt, S. Pitman, Lancaster University, Bailrigg, UK
A. Green, H. Owen, University of Manchester, Manchester, UK

Abstract

Precise proton therapy planning can be assisted by augmenting conventional medical imaging techniques with proton computed tomography (pCT). For adults this requires an incident proton energy up to at least 330 MeV, an energy not readily accessible using cyclotrons. We are presently constructing a prototype of the ProBE 54 MV/m 3GHz post-cyclotron booster linac as a compact method to achieve 330 MeV in the context of the Christie Hospital proton therapy centre, to be tested in the research room there. In this paper, we present beam dynamics studies and tracking simulations of proton beams through the booster region. The longitudinal and transverse particle transmission is calculated from tracking simulations and compared to theoretical models to help understand how best to optimise the optics design through the ProBE region.

INTRODUCTION

The precise dose delivery achievable with proton-based radiotherapy requires accurate treatment planning to obtain the greatest benefit. Presently, margins defined around treatment plan volumes are greater than they might be; these margins account for uncertainties in translating densities from CT scans. Proton CT (pCT) may reduce this error by directly measuring proton stopping via the loss of energy as protons pass completely through an imaged structure; margins could be reduced from as much as 10 mm to as little as 2 mm using this technique, and several proton-counting detector technologies may be employed [1–3]. Whilst head-and-neck and paediatric pCT is within the energy reach of current 230-250 MeV proton therapy machines such as cyclotrons, full adult pCT will require up to 350 MeV protons to maintain the Bragg peak beyond the imaged patient [4, 5]. The Cockcroft Institute is developing solutions to obtain 350 MeV protons using either FFAG or cyclinac approaches [6, 7]. In this paper we discuss the ProBE (Proton Booster Extension) cyclinac which we have proposed as a convenient and compact method to augment the c.250 MeV energies - readily obtainable from modern proton therapy cyclotrons - to the 350 MeV (or higher) required for pCT [8–11]. 350 MeV is judged enough to allow imaging of adults with good density resolution, and our ProBE 3 GHz design will accomplish a 100 MeV increase in energy up to 350 MeV using two 54 MV/m structures in around 3 m when associated beam transport is included. A summary of the ProBE booster parameters is given in Table 1; a fuller description of the cavity design process is given in a separate paper. The delivery of 350 MeV protons to the patient is to be achieved using a novel superconducting gantry concept, also presented at this conference. Visualisations of the prototype cavity design are shown in Figures 1 and 2.

Table 1: Summary of ProBE S-band SC-SWS Booster Linac Parameters

Frequency	3	GHz
Gradient	54	MV/m
Entrance Energy	250	MeV
Exit Energy	350	MeV
Phase Advance	90	deg
Cell Length	29.8	mm
Coupling Factor	2	%
R_S/L	76	MΩ/m
$\sqrt{S_c}/E_{acc}$	2.4×10^{-2}	$\sqrt{\text{W}}$/MV
H_{pk}	254	kA/m
E_{pk}	200	MV/m

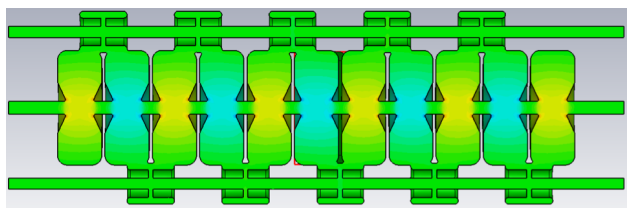

Figure 1: Cutaway view of the ProBE 11-cell prototype cavity presently being manufactured. This is a 3 GHz, 54 MV/m side-coupled standing-wave structure to demonstrate acceleration from 250 MeV upwards.

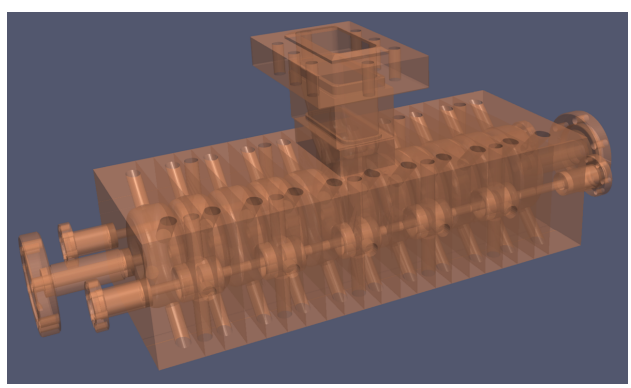

Figure 2: Visualisation of the ProBE 11-cell cavity prototype, showing RF coupler (above), additional access apertures for bead-pull tests (ends) and for tuning studs (below).

* r.apsimon@lancaster.ac.uk

TRANSMISSION AND LOSS

The Cyclinac Method

All cyclinacs - the coupling of a cyclotron source to a downstream linear accelerator - have to cope with the same basic issue of inherent frequency mismatch between the rather low frequency of the cyclotron (set by the magnetic field) and the rather high frequency of the linac (determined in large part by the availability of power sources). For example, the Christie Varian ProBeam cyclotron will have a magnetic field that varies from 2.4 T (central) to about 3.0 T (extraction) to achieve a 72.8 MHz extracted bunch frequency on the 2nd harmonic; this corresponds to a bunch separation of around 13.7 ns, much higher than the 0.33 ns bucket separation even in an S-band linac. The mismatch accounts for a significant fraction of the ~90% particle loss in cyclinacs as the bunches from the cyclotron are accelerated in the linac, the balance of losses coming from the inherent restrictions of the transverse aperture acting on the ~10 mm-mrad emittance from the cyclotron. However, these losses are quite tolerable as the eventual maximum required average current for treatment is only around 10 nA; the losses should also be compared with those obtained when degrading a ~ 800 nA cyclotron current from 250 MeV down to 70 MeV for shallow treatments, which is as much as 99.9%. Cyclinacs used for imaging need only supply a few pA of average current to obtain a useful image in about a minute [12], so losses in this case are even less an issue; more important is a compact size.

Transverse and Longitudinal Transmission

The total particle transmission through any beam line will involve transverse and longitudinal losses, with the total transmission given as the multiple of both

$$T_{total} = T_{trans} \times T_{long} \tag{1}$$

where T_{trans} and T_{long} are the transverse and longitudinal transmission efficiencies respectively. For static beam lines, the transverse and longitudinal transmissions can be considered as independent of each other. By comparing tracking simulations with and without a momentum spread, the transverse and longitudinal losses can be distinguished explicitly.

For RF systems, such as linacs, the transverse and longitudinal transmissions are coupled and the notion of transverse and longitudinal loss is no longer well-defined. The transverse and longitudinal fields experienced by the beam depends on the RF phase, hence the longitudinal position of the particle.

In the following studies, we assume that the particle beam from the cyclotron is Gaussian distributed in x, x', y, y' and $z' = \delta p/p$. For z we assume a uniform distribution because the cyclotron bunch frequency is much lower than that of the booster. Since the bunch length after the cyclotron is approximately 7 booster RF wavelengths, where the wavelength is approximately 5 cm, we only need to simulate a bunch length of one RF wavelength to model all cavity bunch phases.

Figure 3: Diagram of the linac optics showing the RF cavities (brown) and the permanent magnet quadrupoles (red).

Analytical Form of Transmission

For the theoretical transmissions, we will neglect coupling between the transverse and longitudinal phase space as this is caused by dispersive or nonlinear terms in the beam transport map, which are expected to be small.

Longitudinal Transmission In a cyclinac, the fractional momentum spread of the beam at the extraction point of the cyclotron is ~ 1%; through the linac, the momentum spread will be of the order of 20%. As such, we assume that the final momentum distribution of the beam is independent of the initial momentum spread. Since we assume that the longitudinal position of particles is uniformly distributed over one RF cycle, the longitudinal transmission is simply the ratio of the range of stable phases to total phase range of 360 degrees. The range of stable phases, known as the RF bucket, is given by the inequality

$$\phi \cos\phi_s - \sin\phi \leq -(\phi_s \cos\phi_s - \sin\phi_s)\,. \tag{2}$$

For the ProBE cavities, we assume a synchronous phase of $\phi_s = 20°$ [13].

Transverse transmission If we consider the fields in an RF cavity, averaged over all phases, it can be treated as a drift length. For ProBE, a FODO lattice has been chosen as the quadrupole arrangement between cavities in the linac [13] (Figure 3). The normalised phase space acceptance is given as

$$A = \beta\gamma\frac{r_{app}^2}{L} \tag{3}$$

where β and γ are the relativistic parameters, r_{app} is the aperture and L is the distance between quadrupoles.

If we assume that the transverse aperture is a rectangle with limits in x and y of $\pm a_x$ and $\pm a_y$ respectively, and that the transverse beam distribution is Gaussian, then the transverse transmission becomes

$$T_{trans}\,[rect] = \mathrm{erf}\left(\frac{a_x - \mu_x}{\sqrt{2}\sigma_x}\right)\mathrm{erf}\left(\frac{a_y - \mu_y}{\sqrt{2}\sigma_y}\right) \tag{4}$$

where μ_x and μ_y are the offsets and σ_x and σ_y are the beam sizes in the horizontal and vertical directions respectively. The rectangular aperture is chosen as is is one of the few geometries which has a simple analytical solution.

If $a \lesssim \sigma$, then the particle distribution within the aperture is approximately uniform. For other geometries, such as a circular or elliptical aperture, we shall assume that the transmission is the proportional to the area of the aperture as shown in Eq. (5).

$$T_{trans}\,[round] = \frac{\pi}{4}T_{trans}\,[rect] \tag{5}$$

Tracking Simulations

Tracking simulations were undertaken in ASTRA to cor pare to the analytical results. The tracking simulations wei undertaken through a 7-cavity linac using the optics d scribed in Figure 3 in order to determine the transmissio through a booster linac rather than a single cavity. Two se of tracking simulations were run. In the first set of trackin simulations, the transverse and longitudinal dynamics ai treated as uncoupled and modeled separately. The secon simulation tracked the full 6D phase space to study couplin between the transverse and longitudinal planes.

The uncoupled dynamics simulation has been adopte by some designers as it is easy to set up the simulatior and analysis and requires relatively few macroparticles, e. around 10^4. To determine the transverse transmission, tracking simulation is run where the bunch has a realisti transverse distribution, but all particles have the same initi longitudinal position and momentum. To determine the lo gitudinal transmission, the bunch is simulated with a realistic longitudinal distribution, but all particles lie on axis. The disadvantage of the uncoupled method is that the simulated system is neither physically realistic nor representative of the actual system. For the full 6D simulation, a physically realistic bunch is modelled and tracked. However, the tracking simulations require significantly more particles ($\geq 10^6$) than for the uncoupled phase space simulations. For small apertures, the transverse transmission is very low, therefore a large number of particles is required to provide sufficient statistics to calculate the longitudinal transmission as well as the transverse.

To determine the transverse transmission in the full 6D simulation, particles which exceed the aperture through the linac are cut from the distribution, next the longitudinal transmission is determined as the number of remaining particles which also fall outside of the energy acceptance (which is assumed to be ±1 MeV in this analysis). This analysis does not allow us to distinguish between transverse losses or losses due to a coupling of transverse and longitudinal dynamics. As a result, the longitudinal transmission will be overestimated as some of the longitudinal losses (mostly due to under-/over-focusing in the quadrupole magnets) will be mistakenly counted as a transverse loss.

Figure 4 shows the comparison of transmission vs. cavity iris aperture for the tracking simulations and the theoretical model. For small apertures, the analytical method overestimates the transverse transmission because all cavity fields are neglected; for a small aperture, even a small transverse field can deflect a particle into the aperture and so more losses are expected in the tracking simulations. As expected, the 6D tracking simulations show a lower transverse transmission than predicted by the uncoupled phase space tracking due to coupling between the transverse and longitudinal phase spaces.

For the longitudinal transmission, the transmission for the 6D tracking is larger than predicted by the analytical model and the uncoupled simulations. This is because some of the longitudinal losses have been counted as transverse losses.

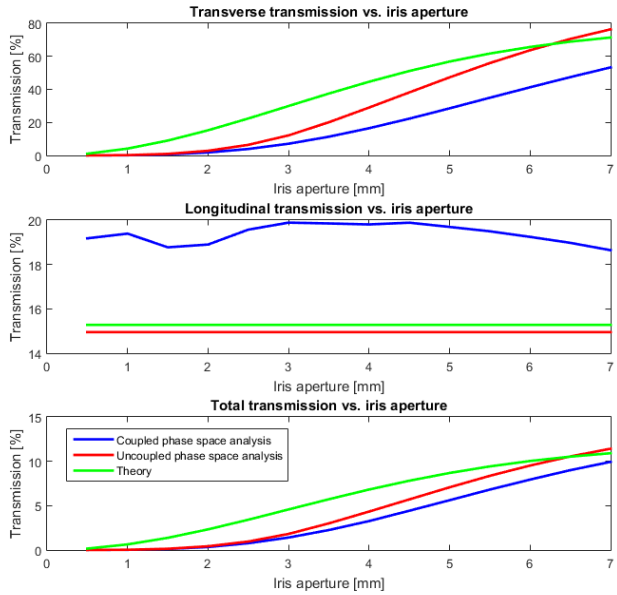

Figure 4: Transverse, longitudinal and total particle transmission vs cavity iris aperture.

For the total transmission, we see that the uncoupled phase space simulations predict a greater transmission than the coupled simulations.

FUTURE PLANS

Further studies are ongoing in order to improve the theoretical understanding of the coupling between transverse and longitudinal dynamics. A model of the transfer map through an RF cavity is being modeled and used to determine the dispersion and nonlinear terms which give rise to this coupling. From this, we aim to understand what affects this coupling and how best to mitigate this. The analytical method generally overestimates the transmission, but this is due to the assumptions and simplifications used. By using a more sophisticated model, it is expected that the analytical model would better agree with the tracking simulations. The uncoupled tracking simulation also overestimates the transverse transmission as well as the total transmission by neglecting coupling between the transverse and longitudinal beam dynamics. Previous methods have been too optimistic in determining the transmission and it is clear that coupling between the transverse and longitudinal phase spaces has a small but important effect.

REFERENCES

[1] K. M. Hanson *et al.*, *Phys. Med. Biol.* 26(6), 965 (1981).

[2] R. W. Schulte *et al.*, *IEEE Trans. Nucl. Sci.* NS-51 (3), 866 (2004).

[3] R. W. Schulte *et al.*, *Med. Phys.* 32(4), 1035 (2005).

[4] H. Owen, R. Mackay, K. Peach, and S. Smith, *Contemp. Phys.* 55(2), 55-74 (2014).

[5] H. Owen, A. Lomax, and S. Jolly, *Nucl. Inst. Meth.* A 809, 96 (2016).

[6] C. Johnstone, H. Owen, and P. Snopok, "A CW FFAG for proton computed tomography", in *Proc. IPAC'12*, New Orleans, LA, USA, paper THPPR053 (2012).

[7] J. Garland, R. B. Appleby, H. L. Owen, and S. Tygier, *PRSTAB* 18, 094701 (2015).

[8] J. A. Clarke, D. M. Dykes, C. W. Horrabin, A. Kacperek, B. Marsland, H. L. Owen, M. W. Poole, S. L. Smith, and V. P. Suller. "Assessing the Suitability of a Medical Cyclotron as an Injector for an Energy Upgrade", in *Proc. EPAC'98*, Stockholm, Sweden, (1998).

[9] U. Amaldi *et al.*, *NIM* A 521, 512 (2004).

[10] A. Garonna *et al.*, *J. Inst.* 5, C09004 (2010).

[11] C. Ronsivalle *et al.*, *Europhys. J. Plus*, 126, 68 (2011).

[12] G. Poludniowski, N. M. Allinson, T. Anaxagoras, M. Esposito, S. Green, S. Manolopoulos, J. Nieto-Camero, D. J. Parker, T. Price, and P. M. Evans, *Phys. Med. Biol.* 59(11), 2569 (2014).

[13] R. Apsimon *et al.*, "ProBE – Proton Boosting Extension for Imaging and Therapy", in *Proc. IPAC'16*, Busan, South Korea, paper TUPOY025, DOI: 10.18429/JACoW-IPAC2016-TUPOY025 (2016).

ISBN 978-3-95450-182-3